

# Extraction of height information from target shadow for applications in ATC

Tan Hwee Pink, Umaiyal Ramanathan  
 Defence Science Organisation National Laboratories  
 20 Science Park Drive Singapore 118230

Telephone 65 8712305/8712294 / Fax 65 8724366 / email : [thweepin@dso.org.sg](mailto:thweepin@dso.org.sg) , [rumaiyal@dso.org.sg](mailto:rumaiyal@dso.org.sg)

*Abstract* – Physical attributes e.g. length and width of a target can be extracted from its radar signature for target characterization. However, an additional dimension i.e. height can provide value added information to distinguish between targets e.g. between Tanks and APCs, which may have similar lengths and widths and which exhibit similar intensity characteristics. For a non-interferometric data collection system, the height of a target can be accurately extracted from its shadow at low grazing angles, fine resolution and a cluttered background.

## 1. INTRODUCTION

Automatic target recognition (ATR) usually comprises 2 phases, training and testing. For feature-based ATR, during the training phase, useful features are measured from signature of known targets from a given class to characterize this target class. This training is performed for all target classes for which the ATR system desires to classify. In the testing phase, feature measurements are performed on the test signature. The unknown target is then classified to the class for which the measurements are closest to.

Feature measurements are usually performed on the target region, and the accuracy relies heavily on the fidelity of the target detection and segmentation algorithms, which have been known to be notoriously unreliable. In addition, the process also exploits only a small fraction of the information in the image.

In fact, an image of a target chip typically comprises 3 regions, namely the target signature, the surrounding clutter as well as the shadow due to the target height, as illustrated in Fig. 1. Unlike the target signature, which is complex and comprises a composite of scatterer responses, the shadow is an almost homogenous noise-like contiguous region. Hence, it will be easier and more accurate to segment the shadow region from the rest of the image, from which useful features can be measured to complement those obtained from the target signature. The height profile along the azimuth is one such useful feature that can contribute to improving the target characterization process. This forms the motivation for our study in this paper.

## 2. REGION SEGMENTATION USING KOLMOGOROV-SMIRNOV DISTANCE<sup>[1]</sup>

In our study, given a target chip, it is desirable to partition the

shadow region from the rest of the image. These 2 regions are visually distinct and exhibit different statistical characteristics. This can be exploited by the Kolmogorov-Smirnov distance, which is a measure of separation between 2 probability distributions and is well known in statistics.

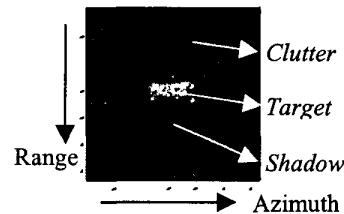


Fig. 1 : Illustration of the various regions in a target chip

### 2.1 Label representation

Many problems in image analysis involve representation of the observed data (gray level SAR image in this case) in terms of label variables. Each pixel in the gray level image is assigned a number, called a label (binary in this case, where '1' for shadow and '0' for non-shadow regions). A label is associated with a pixel according to the statistical properties of its surrounding neighborhood ( a block), as illustrated in Fig. 2. The size of the block must be large enough to capture the statistical properties of the area.

### 2.2 The Kolmogorov-Smirnov (KS) Measure

Consider 2 sets of data,  $v^{(1)} = \{v_1^{(1)}, v_2^{(1)}, \dots, v_{n_1}^{(1)}\}$  and  $v^{(2)} = \{v_1^{(2)}, v_2^{(2)}, \dots, v_{n_2}^{(2)}\}$ , where  $v^{(1)}$  is the gray level of the block of pixels extracted from the shadow region and  $v^{(2)}$  is a distinct block of pixels from another region, as illustrated in Fig. 3.

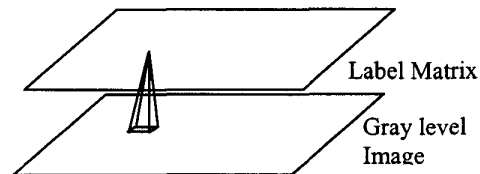


Fig. 2 : Relationship between a label matrix and its associated gray level image

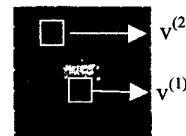


Fig. 3 : Defining 2 regions to compute KS measure

The sample distribution function of a data set  $v = \{v_1, v_2, \dots, v_n\}$  is given in (1)

$$F(t) = \frac{1}{n} \# \{k : v_k \leq t\} \quad (1)$$

The dissimilarity between the 2 data sets, statistically, can be determined using the KS distance, defined as the maximal (vertical) distance between the graphs of  $F^1(t)$  and  $F^2(t)$  in (2)

$$d(v^{(1)}, v^{(2)}) = \max |F^1(t) - F^2(t)| \quad (2)$$

This is illustrated in Fig. 4.

### 2.3 Extraction of shadow from target chip

A reference block is selected within the shadow region. A test block is defined about a test pixel, beginning at the edge of the image. The label associated with the test pixel is obtained by checking the KS measure between the 2 blocks against a threshold,  $K$  as shown below :

$$\text{If } d(\text{ref\_block}, \text{test\_block}) < K, \text{label}(\text{test\_pixel}) = 1 \\ \text{else label}(\text{test\_pixel}) = 0$$

This is repeated by moving the test block over the image in a sliding window approach and the outcome is a binary label matrix. It is possible that small regions of clutter may also be mistakenly classified as shadow pixels, owing to a slight overlap between the clutter and shadow statistics. The true shadow block can then be easily isolated from the other clutter blocks by choosing the largest cluster. Fig. 5 shows an example of such an extraction.

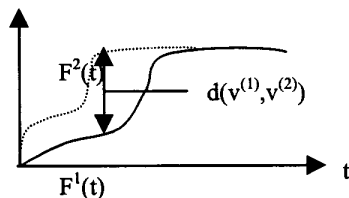


Fig. 4 : Computation of KS measure

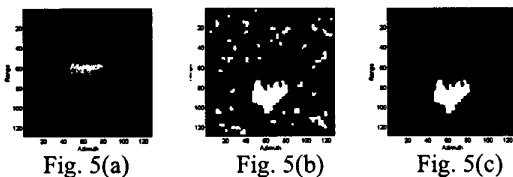


Fig. 5: (a) Original target chip (b) Binary image after KS Segmentation (c) Extracted shadow cluster

### 3. TARGET EXTRACTION USING ADAPTIVE THRESHOLDING

From Fig. 5c, we see that the KS segmentation method fails to extract the shadow accurately in the region close to the far edge boundary of the target. This is due to the merging of target statistics with the shadow statistics in that area.

In order to trace the shadow boundary accurately, it is thus necessary to extract the target region of the chip. The difference in range between the far-edge boundary of the shadow and the target can then be used to calculate the actual length of the shadow, as shown in Fig. 6.

The target region at the centre of the chip is extracted based on adaptive thresholding techniques as shown in Fig. 7. An example of the results after extraction is shown in Fig. 8

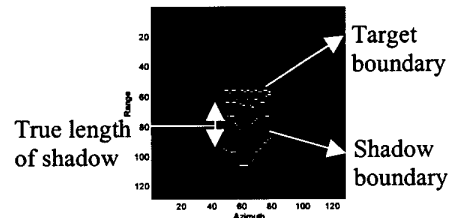


Fig. 6 : Extraction of target and shadow boundary

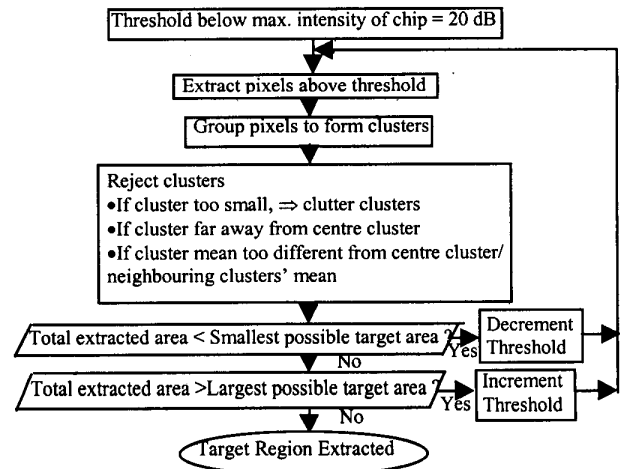


Fig. 7 : Target Extraction Block Diagram



Fig. 8(a) Original Target Chip Fig. 8(b) After Target Extraction

#### 4. HEIGHT PROFILE CALCULATION FROM TRUE SHADOW BOUNDARY EXTRACTION

Once the target and shadow regions have been extracted, their boundaries are extracted. The true extent of the shadow is then defined from the far edge boundary of the target to that of the shadow, as explained in Fig. 6. Voids that pose discontinuities in the boundaries are filled using the values of their nearest neighbours.

Based on image collection geometry, the height of the target at each azimuth location,  $h$ , can be computed, as illustrated in Fig. 8, using (3) :

$$h = L \sin \theta \quad (3)$$

where  $L$  is the length of the shadow and  $\theta$  is the grazing angle. The height profile along azimuth is obtained by applying (3) along the azimuth profile of the shadow region.

#### 5. TEST DATA

The algorithms were tested using the MSTAR public domain database collected by Sandia National Laboratory and released in 1997. The images are collected at 17 degree grazing angle with 1 ft resolution. The range pixel size is 0.2021m and azimuth pixel size is 0.2031m. The target classes available are the T72(Tank) , BTR70(APC) and BMP2(APC). Images used in the analysis have aspect close to broadside, with a maximum deviation of 5 degrees.

#### 6. RESULTS

The height profiles obtained for the various target classes at various aspects close to broadside are shown in Fig. 10. For the same target, slight deviations in the profile are observed owing to inaccuracies in extraction of the shadow boundaries and slightly differing aspect angles.

Two important observations can be made from the height profile plots. First, a unique height profile exists for each target. The height profile of T72 appears steeper than that of BTR70, whose profile appears flatter, while that of BMP2 has an abrupt ascent close to the centre. Secondly, the T72 is taller than the APCs. Eliminating the anomalous results, the maximum height reached by T72 is 2.60m. The maximum height measured for the BTR70 is between 2.07m and 2.19m, while that for BMP2 is between 2.19 and 2.42m.

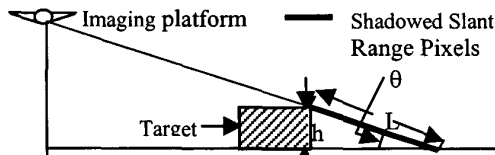


Fig. 8 : Radar Imaging Geometry

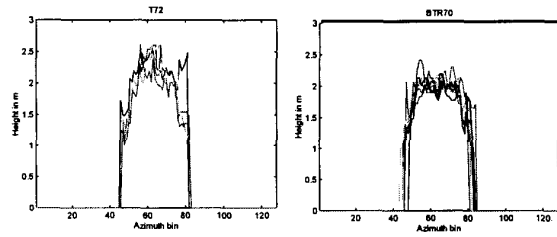


Fig. 10a : Ht profile for T72 Fig. 10b : Ht profile for BTR70

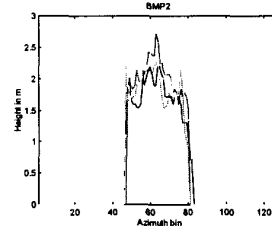


Fig. 10c : Height profile for BMP2

#### 7. CONCLUSION AND RECOMMENDATIONS

Height profile of various target classes was obtained by measuring the length of their shadows. These shadows were extracted quite accurately using Kolmogorov-Smirnov segmentation techniques and adaptive thresholding techniques. The height profiles were found to be unique for the classes investigated. It was found that the maximum height and shape of the height profile could be used to distinguish the T72 from the BTR70 and BMP2.

With these conclusions, it can be inferred that the height profile extracted from the shadow of targets can be used for target classification and discrimination. The requirements are that the imaging is performed at low grazing angles, fine resolution and a cluttered background. With a substantial level of discrimination available at a grazing angle of 17 deg, it is expected that the performance would improve at even lower grazing angles, where shadows are more prominent.

The problem of extracting the height profile for targets at aspects off broadside is more complicated. The equations defining the relationship between the length of shadow and height of target are now influenced by the aspect angle as well. The current height profile extraction algorithms have to be modified to cater for all aspect angles of the target.

#### REFERENCES

- [1] D. Geman, S. Geman, C. Graffigne and P. Dong, "Boundary Detection by Constrained Optimization", IEEE Trans. Pattern Anal. Machine Intell., vol. 12, pp. 609-628, July 1990